

Statistical properties of the noisy on - off intermittency

This article has been downloaded from IOPscience. Please scroll down to see the full text article.

1996 J. Phys. A: Math. Gen. 29 11

(<http://iopscience.iop.org/0305-4470/29/1/005>)

View [the table of contents for this issue](#), or go to the [journal homepage](#) for more

Download details:

IP Address: 171.66.16.68

The article was downloaded on 02/06/2010 at 03:13

Please note that [terms and conditions apply](#).

Statistical properties of the noisy on–off intermittency

A Čenys†‡ and H Lustfeld†

† Institut für Festkörperforschung, Forschungszentrum Jülich, D 52425 Jülich, Germany

‡ Semiconductor Physics Institute, LT-2600 Vilnius, Lithuania

Received 3 February 1995, in final form 22 September 1995

Abstract. The dependence of the escape time on the deviation from the critical point is investigated for the noisy on–off intermittency. The power-law scaling behaviour is destroyed by the noise in a wide region above the critical point. In the general case the width of the region decreases logarithmically with the decrease in the noise amplitude. Below the critical point the noise induced escape time is sensitive to the statistical properties of the chaotic driving signal. Universal exponential dependence holds only for the Gaussian approximation.

1. Introduction

A particular case of an intermittent bursting, recently called on–off intermittency [1], has been predicted for chaotic dynamical systems [2, 3]. A distinguishing feature of dynamical systems having this type of intermittent behaviour is the existence of a smooth invariant manifold in the system's phase space. Below the critical value of a control parameter the dynamics of such a system is chaotic, but completely confined to the smooth manifold having integer dimension less than the dimension of the phase space. At the critical parameter value the smooth manifold loses its stability and blow-out bifurcation takes place [4]. Correspondingly the dynamics starts to depend essentially on the structure of the phase space far from the manifold. If there is a stable attractor outside the manifold, trajectories leaving the unstable repeller on the manifold are to be confined to this other attractor. The intermittent bursting does not occur in this case of hard [2] or hysteretic [4] blow-out bifurcation. However, if there are no stable attractors outside the manifold, the trajectories leaving the vicinity of the manifold can return after some time. The dynamics of the system in this case of soft or non-hysteretic bifurcation consists of short excursions to the outside regions of the phase space and of long 'laminar' phases during which the trajectory stays close to the manifold. While being related to the specific structure of the phase space, on–off intermittency has some common features with both Pomeau–Manneville [5] and crisis induced chaos–chaos intermittency [6, 7]. First, it can be considered as a chaos–chaos intermittency, since the dynamics during the 'laminar' phases, as well as during chaotic bursting, is chaotic. Second, choosing the distance from the invariant manifold as a dynamical observable, the dynamics looks like fixed point to chaos intermittency. This choice is natural in the case of synchronization of identical chaotic systems. In a typical experiment such as that of spin–wave instabilities [8] this particular observable does not correspond to any of the experimentally given observables. In these situations phase space reconstruction can be necessary to detect intermittent behaviour which is not obvious from the 'natural' observables. Such sensitivity to the choice of variables is typical for chaos–chaos intermittency.

On–off intermittency is expected to be a common phenomenon in dynamical systems having a symmetry such as coupled identical maps [2,3], chaotic driving [9], chaotic synchronization [10] or maps generating identical attractors [11]. When using special coordinates all these discrete time systems can be represented in the following form:

$$r_{n+1} = g(x_n)r_n + O(r_n^2) \quad (1)$$

$$x_{n+1} = F(x_n) + O(r_n). \quad (2)$$

In this representation the variables r_n and x_n define the distance from the smooth invariant manifold $r_n = 0$ and the dynamics on the manifold respectively. In the general case both r_n and x_n can be vectors. A particular case of the equations (1) and (2) with continuous time dependence has been studied in [4]. Similar intermittent bursting can also be observed in the case of random maps [12, 13] or multiplicative random driving [9]. In the latter case the dynamical driving $g(x_n)$ in equation (1) is replaced by a random signal.

In previous work on the statistical properties of the on–off intermittency the main attention was concentrated on the estimation of the distribution of the variable r_n [2, 3, 14] or the size and dimension of the snapshot attractors in the case of random maps [12, 13]. Only recently the first results on the statistical properties of the laminar phase lengths, usually estimated in experiments with intermittent dynamics, have been presented [9]. It was shown analytically for the random uncorrelated driving and numerically for chaotic driving that the average of the duration of the laminar phases depends on the deviation from the critical point $|v - v_c|$ via the power law $\langle \tau \rangle \sim |v - v_c|^{-1}$. The distribution of the durations of the laminar phases shows power-law behaviour as well, with an exponent $-3/2$. The same exponents characterize Pomeau–Manneville type III intermittency in the case of a cubic nonlinearity and uniform reinjection. Chaos–chaos intermittency with the statistical properties of type III intermittency has been detected in the spin–wave experiment [8]. This seems to be the first experimental observation of the on–off intermittency. Electronic circuit experiments with external random driving have also been reported recently [15].

For the experimental identification of the on–off intermittency it is very important to know the statistical properties in the noisy case, hence a small random noise is added to equation (1). In coupled nearly identical systems the small differences between the systems also lead to the small additional term in equation (1) with the chaotic ‘noise like’ dynamics [14]. The distribution of the durations of the laminar phases for the noisy on–off intermittency has recently been calculated numerically and discussed by Platt *et al* [16]. Characteristic times of the exponential decay in the distribution function have been estimated analytically by Ott *et al* [17]. Another important characteristic that can be estimated in an experiment is the dependence of the averaged laminar phase duration on the control parameter and on the noise level. It is determined by the properties of the escape time τ . In this paper we present a detailed analysis of these dependences for the noisy on–off intermittency and show that both parameters are relevant. In section 2 the model is described. Analytic results for the Gaussian approximation of the driving signal based on the Fokker–Planck equation are presented in section 3. Numerical examples for various chaotic driving signals given in section 4 show that deviations from the Gaussian distribution are important for the noise-induced metastability below the critical point. An estimate of the escape time for the non-Gaussian case and conclusions are given in section 5 and section 6, respectively.

2. The model

We will investigate the dynamical system (1) and (2) in the presence of small additive noise η . For simplicity we consider the model with linear driving $g(x_n) \equiv ax_n$:

$$r_{n+1} = ax_n r_n + \eta_n \quad (3)$$

$$x_{n+1} = F(x_n) \quad (4)$$

which contains all essential features of noisy on–off intermittency. (A more complicated driving function $g(x_n)$ will be used in two numerical examples presented below.) Equation (3) can be considered as a dynamical system driven by two stochastic forces x_n and η_n . In this model stochasticity of the multiplicative driving is related to the chaotic dynamics of the map F and stochasticity of the additive driving is related to the extrinsic noise. The main results of this model, however, are valid also for other models like random maps [12, 13], when both multiplicative and additive driving forces are random. For coupled nearly identical chaotic systems both driving forces are stochastic due to the intrinsic chaotic dynamics of the map F .

The laminar phase duration for intermittent dynamical systems is calculated by averaging the escape time, i.e. the time necessary for the system to pass the threshold r_{th} starting at point $r_0 < r_{\text{th}}$, over the probability of reinjection at r_0 . Small enough values of the threshold r_{th} should be chosen to observe universal scaling properties. In the Pomeau–Manneville case escape time is defined by the type of intermittency and values of r_0 and r_{th} alone, while the reinjection probability depends on the dynamics far from the fixed point and is usually assumed to be uniform. In the case of on–off intermittency the time necessary to pass the threshold r_{th} starting at point $r_0 < r_{\text{th}}$ may vary strongly due to dependence on the realization of the driving signal x_n . The dynamics of the variable r_n is more similar to a random walk or diffusion than to a deterministic process. In this situation the escape time is the *first passage time* [18], i.e. an appropriate average over the ensemble of the times needed to pass from r_0 to r_{th} .

The diffusional process of the linear equation (3) will also describe reinjection to the region below threshold $r < r_{\text{th}}$. For small threshold values this linear process completely determines the reinjection probability and nonlinear terms are important only to ensure the boundedness of the system. It is natural in this case to assume that the probability of the reinjection is concentrated in the narrow region close to the threshold. This assumption becomes invalid only for large amplitude of the driving signals x_n . Moreover, as will be shown later, the escape time—apart from exponential tails—depends on r_0 only in a non-sensitive way, namely via $\ln r_0$. Therefore we may write for the escape time when averaged over the reinjection probability

$$\langle \tau \rangle \approx \tau(r^*) \quad r^* = \exp\{\langle \ln r_0 \rangle\} \quad (5)$$

where r^* is close to the threshold value r_{th} . As a result this averaged escape time will show generically the same structure as the escape time for a given r_0 .

Additive noise η_n in equation (3) dominates for small r_n and can be neglected for large r_n . The most important consequence of the presence of noise is that the noisy system cannot stay at the noise-free fixed point $r_n = 0$. A simple way to model the influence of additive noise [16], is to add a reflecting barrier at the small level r_b proportional to the noise amplitude. Replacement of the noise term η_n by a boundary condition allows us to use the methods of analysis similar to those which have been used earlier in the noiseless case [2, 3, 14]. Introducing the logarithmic variable $y_n = \ln |r_n|$, equation (3) becomes

$$y_{n+1} = y_n + \ln |x_n| + \ln |a|. \quad (6)$$

It follows from equation (6) that the critical parameter value is

$$|a_c| = \exp(-\lambda) \quad (7)$$

where $\lambda = \langle \ln |x_n| \rangle$ with $\langle \dots \rangle$ denotes the time average. In the case of coupled identical one-dimensional maps one has $g \equiv a dF/dx$ in equation (1) and λ corresponds to the Lyapunov exponent of the single map.

Close to the critical point $v = (a - a_c)/a_c \ll 1$, equation (6) can be rewritten as

$$y_{n+1} = y_n + v + \beta_n \quad (8)$$

where the new variable $\beta_n = \ln |x_n| - \lambda$ has zero mean value $\langle \beta_n \rangle = 0$. Map (8) represents a biased ‘chaotic’ walk [9] where β_n is a chaotic variable, usually exponentially decaying but still having finite correlation length. Close to the critical point typical escape times are large and completely determined by the long time behaviour. This behaviour can be obtained from the N th iteration of the map (8) which has the same form as the original one with a properly rescaled y_n and the driving variable

$$\Lambda_n = N^{-1} \sum_{k=1}^N \beta_{nN+k}. \quad (9)$$

For large N the variables Λ_n can be assumed to be uncorrelated and to have—according to the central limit theorem—a probability distribution [19]

$$P_N(\Lambda) \sim e^{N\Psi(\Lambda)}. \quad (10)$$

For many driving systems the distribution $P(\Lambda)$ can be approximated by a Gaussian distribution corresponding to $\Psi(\Lambda) = -\Lambda^2/2D$ with $D = \lim_{N \rightarrow \infty} (N \langle \Lambda^2 \rangle)$. The escape time for the Gaussian driving can easily be calculated using standard methods. This will be done in the next section. The non-Gaussian case is discussed in section 5.

3. The Gaussian case

For analysing the long time behaviour the map (8) is replaced by the corresponding stochastic differential equation. Assuming uncorrelated Λ_n and a Gaussian distribution of $P(\Lambda)$, the time-dependent probability density f of the variable y_n satisfies the Fokker–Planck equation

$$\frac{\partial f}{\partial t} = -v \frac{\partial f}{\partial y} + \frac{D}{2} \frac{\partial^2 f}{\partial y^2}. \quad (11)$$

To calculate the escape time for a given y_0 equation (11) is solved with the initial condition

$$f(t = 0, y) = \delta(y - y_0). \quad (12)$$

One boundary condition is obtained by requiring that f vanishes at the threshold

$$f(t, y = y_{\text{th}}) = 0 \quad (13)$$

where $y_0 = \ln r_0$ and $y_{\text{th}} = \ln r_{\text{th}}$. The other boundary condition is obtained by incorporating the random noise of equation (3). This requires a reflecting barrier[16], i.e. zero flow at $y_b = \ln r_b$:

$$J(t, y = y_b) \equiv -vf + D/2 \frac{df}{dy} = 0 \quad (14)$$

where r_b characterizes the noise amplitude ($r_b < r_0 < r_{\text{th}}$). Now the escape time is obtained from the probability density via†

$$\tau = - \int_0^\infty dt \int_{y_0}^{y_{\text{th}}} dy \frac{\partial}{\partial t} f(t, y) = \int_{y_0}^{y_{\text{th}}} dy \int_0^\infty dt f(t, y) \quad (15)$$

† In [18] the escape time is synonymous for *first passage time*.

and is easily determined since we do not need f itself but the time integral of f only. Integrating equation (11) over t and using $f(\infty, y) = 0$ we end up with a linear ordinary differential equation for $h(y) = \int_0^\infty dt f(t, y)$. Solving it we get the analytic expression for the escape time

$$\tau = \frac{z_0}{v} + \frac{D}{2v^2} e^{-2vz_b/D} (1 - e^{2vz_0/D}) \quad (16)$$

where $z_0 = y_{\text{th}} - y_0 \equiv \ln(r_{\text{th}}/r_0)$ and $z_b = y_{\text{th}} - y_b \equiv \ln(r_{\text{th}}/r_b)$. According to considerations presented in section 2, the averaged escape time (i.e. the escape time averaged over reinjection position r_0) will show the same structure as the escape time (16) provided we make the replacement suggested in equation (5). Taking into account that for diffusional reinjection $vz_0/D \ll 1$, three regions of v can be defined which depend on the sign of v as well as on the ratio of the ballistic time τ_b and the diffusion time τ_d . Here the diffusion time $\tau_d = z_b^2/D$ is the time needed by the system to reach the threshold due to diffusion when starting at the noise level. A corresponding interpretation holds true for the ballistic time $\tau_b = z_b/|v|$. Above the critical point ($v > 0$) the condition $\tau_d \gg \tau_b$ defines the ballistic region with negligible diffusion. In this region the escape time depends on v as in the noiseless case:

$$\tau = z_0 v^{-1} \equiv v^{-1} \ln(r_{\text{th}}/r_0). \quad (17)$$

Below the critical point ($v < 0$) one finds noise-induced metastability for $\tau_d \gg \tau_b$. In this noise-controlled region the system stays a long time at the noise level until at last the driving signal brings it to the threshold. The escape time in this case is determined by the exponential tail of the distribution function

$$\tau = -z_0 v^{-1} e^{-2vz_b/D} \equiv -\frac{\ln(r_{\text{th}}/r_0)}{v} (r_{\text{th}}/r_b)^{-2v/D} \quad (18)$$

and it is finite for any finite value of v . This is due to the Gaussian approximation which corresponds to the unbounded driving signal. The shift of the exact intermittency onset due to noise, discussed in [16], is related to the bounded driving signal. However, the escape time in the region of the onset is very long for small noise. The region close to the noiseless critical point is of practical interest in real and even numerical experiments. It should also be pointed out that the exponential dependence of the noise-induced escape time for on–off intermittency is determined by the distribution of the driving signal. It is not sensitive to the distribution of the additive random noise. This is in contrast with the crisis induced chaos–chaos intermittency when statistical properties of the noise are important and only scaling is universal [20].

Exponential noise-induced escape time (18) and noiseless scaling (17) can be detected only outside the crossover region $\tau_d \ll \tau_b$. In the crossover region the escape is determined by diffusion. At the critical point $v = 0$ the escape time

$$\tau = 2z_0 z_b D^{-1} \equiv 2D^{-1} \ln(r_{\text{th}}/r_0) \ln(r_{\text{th}}/r_b) \quad (19)$$

increases to infinity with the decrease of noise r_b only logarithmically. The same slow dependence also characterizes the width of the crossover region

$$v^* = \frac{2D}{z_b} \equiv \frac{2D}{\ln(r_{\text{th}}/r_b)}. \quad (20)$$

The transition between ballistic and noise-controlled regions is smooth in the Gaussian case due to this wide crossover region.

4. Numerical examples

Using equations (3) and (4) the escape time τ was determined numerically by averaging the number of iterations needed for the system to pass the threshold r_{th} after starting from

the initial value r_0 . When passing r_{th} during one run the value of r was reset to r_0 without resetting x of the map F . All results presented below are obtained for the uncorrelated noise η_n in equation (3) uniformly distributed in the interval $[-r_{\text{noise}}, r_{\text{noise}}]$. They are very close to results obtained for the noise with Gaussian distribution.

In the first example the choice for F is the skewed tent map

$$F(x) = \begin{cases} x/p & x \leq p \\ (1-x)/(1-p) & p < x \leq 1 \end{cases} \quad (21)$$

and the choice for the driving signal g is[†] $g \equiv a dF/dx$. Comparison with the analytic results is easy because $\Psi(\Lambda)$, corresponding to the scaling function of the local Lyapunov exponents, can be calculated analytically [19]. For parameter $p = 0.3$ it can be well approximated by a Gaussian parabola with the cut-offs for both positive and negative Λ . Parameter D in (16), corresponding to the dispersion of variable Λ , is calculated numerically from the formulae at the end of section 2. As can be seen from figure 1 the numerically calculated escape time agrees well with formula (16) in a wide region around the critical point. Below the critical point the noise-controlled region with an exponential dependence on v can be detected. An exact agreement cannot be expected due to replacement of the real additive noise by the reflecting boundary condition in the analytic calculation. The proportionality coefficient between the noise amplitude r_{noise} and the barrier position r_b depends on the noise properties and serves as a fitting parameter. The estimated escape time does not depend on the threshold value r_{th} , if starting point r_0 and noise amplitude r_{noise} are rescaled correspondingly. This holds true for the linear structure of equation (3) but it has also been verified numerically for this more general case.

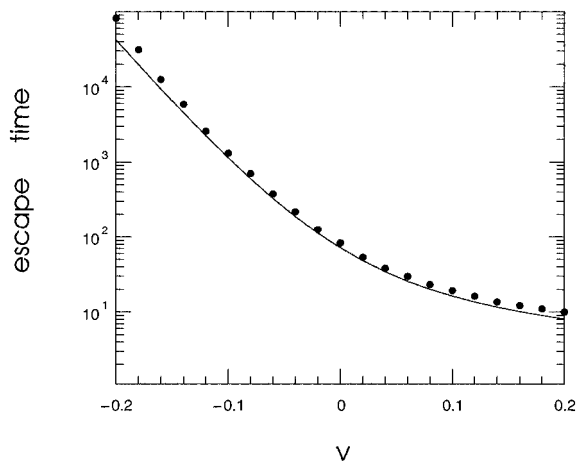


Figure 1. Escape time against the deviation from the critical point, v , for the skewed tent map with $p = 0.3$: starting point $r_0 = 0.001$, threshold value $r_{\text{th}} = 0.005$, noise amplitude $r_{\text{noise}} = 0.0001$. The full curve corresponds to the analytic result (16) with $D = 0.15$.

In the second example we take for F the Henon map $x_{n+1} = 1 + 0.3x_{n-1} - 1.4x_n^2$ and for g the linear map $g \equiv ax_n$. The numerically calculated function $\Psi(\Lambda)$ is shown in figure 2. It can be approximated by a Gaussian parabola with a numerically obtained D only in the narrow region close to the maximum. As a result the escape time can be described only above the critical point by equation (16) valid for Gaussian approximation. This is

[†] This choice of the function g is appropriate when discussing coupled identical one-dimensional maps [14].

shown in figure 3. The noise induced escape time essentially depends on the deviations from the Gaussian distribution. To demonstrate this we have also calculated the escape time for ($g \equiv ax_n^{-1}$ in equation (1)). This corresponds to a changed sign of Λ in $\Psi(\Lambda)$. Considering that the escape time is essentially determined by positive Λ , the correlation below the critical point between $\Psi(\Lambda)$ and the escape time can easily be seen in figure 3.

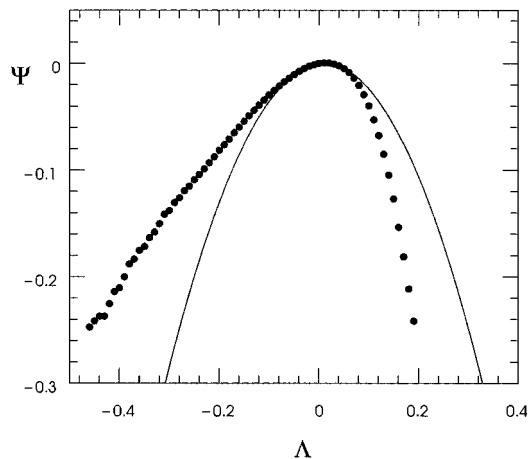


Figure 2. Function $\Psi(\Lambda)$ calculated numerically with $N = 50$ for the Henon map. Close to the maximum it is approximated by the Gaussian parabola with $D = 0.169$.

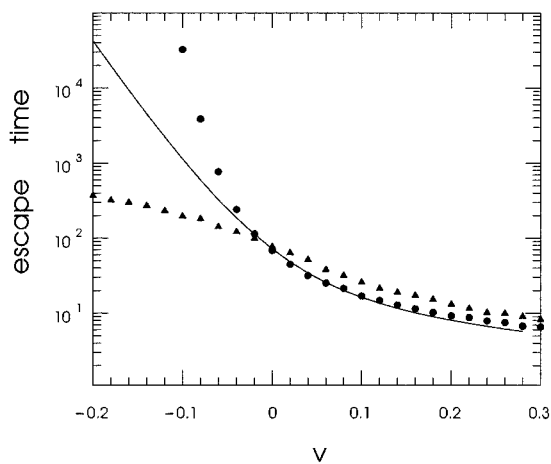


Figure 3. Escape time for the Henon map: dots, driving signal x_n ; triangles, driving signal x_n^{-1} . The full curve corresponds to the analytic result (16).

In the last example we again take for g the linear map and for F the logistic map at fully developed chaos $x_{n+1} = 1 - 2x_n^2$. This yields a non-analytic function $\Psi(\Lambda)$ [21]

$$\Psi(\Lambda) = \begin{cases} -|\lambda| & \Lambda \leq \ln 2 \\ -\infty & \Lambda > \ln 2. \end{cases} \quad (22)$$

Here the distinguishing feature of the escape time as a function of v is a sharp transition between ballistic behaviour above the critical point and noise-controlled behaviour below

the critical point (cf figure 4). In contrast to the Gaussian case the crossover region is very narrow for small noise amplitudes. The peculiarities of the escape time in the non-Gaussian case are discussed in the next section.

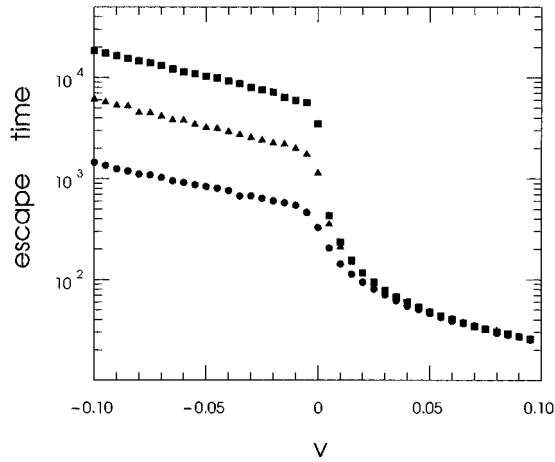


Figure 4. Escape time for the logistic map at different noise amplitudes r_{noise} : dots, 0.001; triangles, 0.0003; squares, 0.0001.

5. The non-Gaussian case

As seen from the numerical examples the noise-controlled regime is most sensitive to deviations from the Gaussian distribution. In this regime v is negative and large enough that starting from the initial point the system quickly reaches the noise level with high probability. The escape time in this case is determined by the small probability to reach the threshold from the noise level due to the driving chaotic signal. Neglecting higher order terms describing probabilities for reaching the threshold more than once or for staying in the region above threshold, probability and escape time can be approximated as

$$\tau^{-1} \sim \sum_{n=1}^{\infty} \int_{(z_b/n)-v}^{\infty} P(\Lambda) d\Lambda. \quad (23)$$

The integral in (23) gives an estimate of the probability to reach the threshold from the noise level after exactly n iterations. Taking into account that the fast decaying function (10) has its largest value at the lower limit of integration and replacing the summation over n by an integration one obtains

$$\tau^{-1} \sim \int_0^{\infty} \exp[n\Psi(z_b/n - v)] dn \sim \exp[n^*\Psi(z_b/n^* - v)]. \quad (24)$$

Here the saddle point value n^* has to be determined from the relation

$$n^*\Psi(z_b/n^* - v) = z_b\Psi'(z_b/n^* - v). \quad (25)$$

For the Gaussian approximation of $\Psi(\Lambda)$ the result of equation (24) together with equation (25) gives the same exponent as obtained from the analysis based on the Fokker–Planck equation, equation (18). However, equation (24) can be applied to the general functions $\Psi(\Lambda)$ including those having a non-analytic maximum. In the case

$\Psi(\Lambda) = -c|\Lambda|^\alpha$ it gives

$$n^* = v^{-1}z_b(1 - \alpha) \quad (26)$$

$$\tau \sim \exp[c\alpha z_b\{\alpha v/(1 - \alpha)\}^{\alpha-1}]. \quad (27)$$

Note that for $\alpha = 2$ the exponent corresponds to that of equation (18).

The above approximation is valid only if the saddle point value n^* is positive and large. For small values of n^* , expression (10) for the probability distribution $P(\Lambda)$ based on the central limit theorem is not valid. Due to this limitation, formula (27) can be applied only for $\alpha > 1$. The numerically studied logistic map represents the marginal case $\alpha = 1$. Since for the logistic map $\Psi(\Lambda)$ has a cut-off at $\Lambda = \ln 2$ it follows from equation (27)

$$\tau \sim e^{z_b(1-v/\ln 2)} \quad |v| \ll \ln 2. \quad (28)$$

Note that an exponential increase of the escape time as a function of v is predicted for negative v . This is confirmed by the numerical calculations presented in figure 4.

The above expressions for the escape time are valid only in the noise-controlled region where the escape time is large. The scaling of the limiting value $|v^-|$ at which the crossover region begins can be estimated from the condition $\tau \sim 1$

$$|v^-| \sim (z_b)^{-1/(\alpha-1)} \equiv (\ln r_{\text{th}}/r_b)^{-1/\alpha-1}. \quad (29)$$

In the ballistic region above the critical point, typical trajectories reach the threshold from the initial point without coming close to the noise level. In this case the escape time depends only on the average exponential growth and details of the probability function are not important. For both Gaussian and non-Gaussian probability distributions the escape time is described by expression (17), valid in the noiseless case. The probability to reach the noise level during the escape is proportional to the probability of finding $\Lambda \leq -v(z_b/z_0 + 1) \approx -vz_b/z_0$. For the above non-analytic function Ψ , according to equation (10) this probability is proportional to

$$e^{-z_b(vz_b/z_0)^{\alpha-1}}. \quad (30)$$

Consequently the limiting value for the ballistic regime $|v^+|$ scales as

$$|v^+| \sim \frac{z_b}{z_0} (z_b)^{-1/(\alpha-1)}. \quad (31)$$

The values v^- and v^+ define the width of the crossover region for the general non-Gaussian case. Now the additive noise amplitude is proportional to r_b . Therefore the width of the crossover region is not a function of the noise amplitude but a function of the logarithm of the noise amplitude. This explains why in the vicinity of the critical point already very small additive noise becomes essential and ensures the smooth transition of the escape time behaviour between the ballistic region and the noise-controlled region. However, for $\alpha \rightarrow 1$ the width of the crossover region goes to zero and one should observe a sharp phase transition like behaviour. This can be seen in figure 4 for the marginal case $\alpha = 1$ of the logistic map. It turns out that in the particular case of the logistic map the crossover region is proportional to the amplitude of small additive noise.

6. Conclusions

In this paper we have studied how the escape time depends on the control parameter for noisy on–off intermittency. We have shown that additive noise, unavoidable in any experiment, is relevant destroying the power-law dependence in a wide region around the critical point. The width of this crossover region decays only logarithmically with the decrease of the noise amplitude. Power-law behaviour with exponent -1 —valid for the noiseless case—can be

observed above the critical point outside the crossover region only. Below the critical point, noise-induced metastability is found. The escape time dependence on the control parameter in this noise-controlled region depends on the statistical properties of the driving chaotic signal. In the case of Gaussian approximation universal exponential dependence can be observed. It is determined by the analytic maximum in the function $\Psi(\Lambda)$. Exponential dependence can be observed for very small noise even if the tails of $\Psi(\Lambda)$ deviate from the Gaussian ones. Escape times have also been estimated in the noise-controlled region for non-analytic functions $\Psi(\Lambda)$.

Acknowledgments

This work was partially supported by ECC (contract No CIPA-CT93-0255). One of us (AČ) wants to thank the DFG for financial support and the Theory 1 group of the IFF, Forschungszentrum Jülich, for hospitality.

References

- [1] Platt N, Spiegel E A and Tresser C 1993 *Phys. Rev. Lett.* **70** 279
- [2] Pikovsky A S 1984 *Z. Phys. B* **55** 149
- [3] Fujisaka H and Yamada H 1985 *Prog. Theor. Phys.* **74** 918; 1986 *Prog. Theor. Phys.* **75** 1087
- [4] Ott E and Sommerer J C 1994 *Phys. Lett.* **188A** 39
- [5] Pomeau Y and Manneville P 1980 *Commun. Math. Phys.* **74** 189
- [6] Grebogi C, Ott E and Yorke J A 1982 *Phys. Rev. Lett.* **48** 1507
- [7] Grebogi C, Ott E, Romeiras F J and Yorke J A 1987 *Phys. Rev. A* **36** 5365
- [8] Rodelsperger F, Weyrauch T and Benner H 1992 *J. Magn. Magn. Mater.* **104–107** 1075
Rodelsperger F, Čenys A and Benner H 1996 *Phys. Rev. Lett.* to appear
- [9] Heagy J F, Platt N and Hammel S M 1994 *Phys. Rev. E* **49** 1140
- [10] Pecora L M and Carroll T L 1990 *Phys. Rev. Lett.* **64** 821
- [11] Čenys A 1993 *Europhys. Lett.* **21** 407
- [12] Yu I, Ott E and Chen Q 1990 *Phys. Rev. Lett.* **65** 2935
- [13] Yu I, Ott E and Chen Q 1991 *Physica* **53D** 102
- [14] Pikovsky A S and Grassberger P 1991 *J. Phys. A: Math. Gen.* **24** 4587
- [15] Hammer P W, Platt N, Hammel S M, Heagy J F and Lee B D 1994 *Phys. Rev. Lett.* **73** 1095
- [16] Platt N, Hammel S M and Heagy J F 1994 *Phys. Rev. Lett.* **72** 3498
- [17] Ott E *et al* 1994 *Physica* **76D** 384
- [18] Stratonovich R L 1963 *Topics in Theory of Random Noise* vol I (New York: Gordon and Breach)
- [19] Eckmann J-P and Procaccia I 1986 *Phys. Rev. A* **34** 659
- [20] Sommerer J C, Ott E and Grebogi C 1991 *Phys. Rev. A* **43** 1754
- [21] Grassberger P, Badii R and Politi A 1988 *J. Stat. Phys.* **51** 135